Chapter 18
Sliding Mode Controllers and Observers for Electromechanical Systems

J. de Leon-Morales

Abstract. Controllers and observers for electromechanical systems are widely used and implemented in the industry in order to improve its performance. Among different electromechanical systems we can find interesting domains of application such as power systems, UAVs, teleoperation. This paper intents to show the advantages of the control and observer design using sliding mode techniques. These domains are related with the research topics of the Mechatronics laboratory of the Nuevo Leon University, in the CIIDIT-UANL Research Institute.

18.1 Introduction

During the last two decades significant interest on sliding mode control has been generated in the research community. The success of sliding mode techniques is the significative performance of the system due to the insensitivity to parameters variations and the complete rejection of disturbances ([13]). However, some challenges are present due to the so-called chattering phenomenon. Several efforts to explain and reduce the effects of the chattering have been done in order to avoid this limitation. The propose of this paper is to provide some illustrative applications of the sliding-mode design which have been developed recently in the Mechatronics laboratory of the CIIDIT-UANL Research Institute ([17], [25], [28], [29]).

An overview of the applications of the sliding modes to electromechanical systems is presented in this work. The control of electrical machines in power systems, UAVs like small helicopters and the most recent applications in teleoperation of the electromechanical systems like a robots or machines, are probably the most challenging topics. We focus on the control of systems using directly or indirectly the theoretical concepts of sliding mode to achieve stability, regulation or tracking.

J. de Leon-Morales
Facultad de Ingeniería Mecánica y Eléctrica
Universidad Autónoma de Nuevo León, Cd. Universitaria,
66450 San Nicolás de los Garza, N.L., México
e-mail: drjleon@gmail.com

L. Fridman et al. (Eds.): Sliding Modes, LNCIS 412, pp. 493–516.
springerlink.com

18.1.1 Application Domains of Sliding Mode

18.1.1.1 Power Systems: Synchronous Machine and Multi-machine Systems

The transient stability of power systems is a classical dynamical control system problem. The application of nonlinear control methods to design the excitation control has been investigated for improving the transient stability of a power system. A survey on power systems control shows that most existing controllers are designed assuming that power systems have fixed structure and constant parameters. However, in power systems uncertainties always exist and they are due to sudden load shedding, generation tripping, occurrence of faults, change of parameters and network configuration among others. These problems are some of the typical conditions found in power systems which must be taken into account for control and observer design (see [11], [12], [14], [16], [17], [18]). In this work, a synchronous machine connected to an infinity bus (SMIB) and a multi-machine system are considered for illustrating the control design using sliding mode techniques to improve the transient stability of such systems.

18.1.1.2 UAV: Twin Rotor System

Recently, a lot of works related with the control of the UAV have been published. The main objective is to design controllers stabilizing UAV's taking into account the perturbations and tracking a specific trajectory. Furthermore, the helicopter is an aircraft that is lifted, propelled and maneuvered by vertical and horizontal rotors. All twin rotor aircraft have high cross-coupling in all degrees of motion. For this reason, this system poses very challenging problem of precise maneuvering in the presence of cross-coupling ([19], [20]). In this work, some results are presented by applying a sliding mode control which is implemented in a setup of a twin rotor system.

18.1.1.3 Teleoperation

The evolution of important technologies and the development of computational tools have allowed the implementation of robotic systems in the industry. Recently, the application of robots in telesurgery and the use the images have permitted to improve accuracy and performance and helping surgeon in complex and delicate surgeries, saving time and money. Furthermore, the stability and transparency are two of the most important topics in teleoperation. In particular, maintain stability of the closed-loop system irrespective of the behavior of the operator or the environment, is one of the most important tasks to be considered if a communication medium (wireless or wired) is included in the scheme. The complexity of the overall system introduces distortion, delays and losses that impact in the stability and performance. Several schemes have been proposed to study such systems, for example those based on passivity, which is inspired in the network theory in transmission lines. However, sliding-mode control has been used extensively in robotics to cope with

parametric uncertainties and hard nonlinearities, in particular for time delay teleoperators, which have gained gradual acceptance due to technological advances. In this work, a scheme to design a sliding mode teleoperator controller to guarantee robust tracking under unknown constant time delay is presented (see for more details [1], [8], [9]).

18.1.2 Paper Structure

The rest of the work is organized as follows. Section 18.2 shows the general ideas of sliding modes techniques used to design an observer and a controller of a power system, where a mathematical model of one machine connected to the transmission line to the infinity bus and multi-machine power system are presented. In Section 18.3, the model of a twin rotor system is presented, where results are given for illustrating the performance of this methodology. Furthermore, using a master-slave configuration, the teleoperation problem is analyzed in Section 18.4. A control scheme using a super twisting algorithm based on sliding-modes is given to solve the bilateral problem which is robust in presence of unknown constant time-delays. Finally, conclusions are presented in Section 18.5.

18.2 Power Systems: Synchronous Machine and Multi-machine Systems

Most of the electrical power systems are operating closer to their technical limits putting restrictions to supply electrical energy to all customers which represent a big challenge to the electrical industry. Conventional controllers based on approximated linearized models are usually tuned at one particular operating point. Nevertheless, due to nonlinear nature of power systems it may be required to be re-tuned when the operating point changes, assuring in this way a satisfactory dynamic performance. Furthermore, in case of severe disturbances, the configuration of power system may be drastically changed. Under such changing conditions, nonlinear controllers offer an alternative to traditional controllers, allowing to improve the performance of power systems under such uncertain conditions. In what follows, we present a control scheme based on sliding mode techniques in order to guarantee the stability under disturbances present in the line or parametric uncertainties.

18.2.1 Synchronous Machine

Although the existing classical controllers have good dynamical performance for a wide range of operating conditions and disturbances, however, the real electric power system have been experimenting a dramatic change in recent years. Because

of that, a lot of attention has been paid to the application of advanced control techniques in power systems as one of the most promising application areas.

In this Section, the control objective is to design a sliding mode controller for a synchronous machine connected to an infinity bus (SMIB) in such a way to regulate the terminal voltage and improve the transient stability of the system over a wide operating region and under external perturbations.

The equations describing the electromechanical transient behavior of a synchronous machine with flux linkage variations, machine damping and transient saliency included are the following

$$\begin{aligned}
\dot{\delta} &= \omega - \omega_s \\
\dot{\omega} &= \frac{\omega_s}{2H}\left(T_M - \frac{X''_d - X_{ls}}{\left(X'_d - X_{ls}\right)}E'_q I_q - \frac{X'_d - X''_d}{\left(X'_d - X_{ls}\right)}\psi_d I_q - \frac{X''_q - X_{ls}}{\left(X'_q - X_{ls}\right)}E'_d I_d \right. \\
&\quad \left. + \frac{X'_q - X''_q}{\left(X'_q - X_{ls}\right)}\psi_q I_q - \left(X''_q - X''_d\right) I_d I_q - D\left(\omega - \omega_s\right)\right) \\
\dot{E}'_q &= \frac{1}{T'_{doi}}\left(-E'_q - \left(X_d - X'_d\right)\left[I_d - \frac{X'_d - X''_d}{\left(X'_d - X_{ls}\right)^2}\left(\psi_d + \left(X'_d - X_{ls}\right) I_d - E'_q\right)\right] + E_{fd}\right) \\
\dot{E}'_d &= \frac{1}{T'_{qo}}\left(-E'_d + \left(X_q - X'_q\right)\left[I_q - \frac{X'_d - X''_d}{\left(X'_q - X_{ls}\right)^2}\left(\psi_q + \left(X'_q - X_{ls}\right) I_q + E'_d\right)\right)\right] \\
\dot{\psi}_d &= \frac{1}{T''_{do}}\left(-\psi_d + E'_q - \left(X'_d - X_{ls}\right) I_d\right) \\
\dot{\psi}_q &= \frac{1}{T''_{qo}}\left(-\psi_q - E'_d - \left(X'_q - X_{ls}\right) I_q\right)
\end{aligned} \tag{18.1}$$

together with the linear algebraic relations between currents and flux linkages:

$$\begin{aligned}
0 &= \left(R_s + R_e\right) Id - \left(X''_q - X_{ep}\right) I_q - \frac{X''_q - X_{ls}}{\left(X'_q - X_{ls}\right)}E'_d + \frac{X'_q - X''_q}{\left(X'_q - X_{ls}\right)}\psi_q + V_s sin\left(\delta - \theta_{vs}\right) \\
0 &= \left(R_s + R_e\right) I_q - \left(X''_d - X_{ep}\right) I_d - \frac{X''_d - X_{ls}}{\left(X'_d - X_{ls}\right)}E'_q + \frac{X'_d - X''_d}{\left(X'_d - X_{ls}\right)}\psi_d + V_s cos\left(\delta - \theta_{vs}\right),
\end{aligned}$$

$$\begin{aligned}
T_e &= \frac{X''_d - X_{ls}}{\left(X'_d - X_{ls}\right)}E'_q I_q + \frac{X'_d - X''_d}{\left(X'_d - X_{ls}\right)}\psi_d I_q + \frac{X''_q - X_{ls}}{\left(X'_q - X_{ls}\right)}E'_d I_d \\
&\quad + \frac{X'_q - X''_q}{\left(X'_q - X_{ls}\right)}\psi_q I_q + \left(X''_q - X''_d\right) I_d I_q
\end{aligned} \tag{18.2}$$

where

$\delta(t)$	Rotor angle, in radians;
$\omega(t)$	Relative speed, in rad/s;
$\omega_s = 2\pi f_s$,	Synchronous machine speed, in rad/s;
H	Inertia constant, in seconds;
D	Damping factor;
T_m	Mechanical power input, in p.u.
T_e	Electrical power output, in p.u.;
E_f	Excitation system voltage, in p.u.
T'_{do}	Open circuit d-axis time constant, in sec;
T'_{qo}	Open circuit q-axis time constant, in sec;
T''_{do}	d-axis sub-transient time constant, in sec;
T''_{qo}	q-axis sub-transient time constant, in sec;
x_d	d-axis synchronous reactance, in p.u.;
x_q	q-axis synchronous reactance, in p.u.;
x'_d	d-axis transient reactance, in p.u.;
x'_q	q-axis transient reactance, in p.u.;
x''_d	d-axis sub-transient reactance, in p.u.;
x''_q	q-axis sub-transient reactance, in p.u.;
$I_q(t)$ and $I_d(t)$	Currents in d-q reference frame of the generator,
$E'_d(t)$	Transient EMF in the direct axis,
$E'_q(t)$	Transient EMF in the quadrature axis,
ψ_d and ψ_q	Flux linkages, direct and quadrature.

where p.u. stands per unit.

18.2.2 One Axes Model

In power systems, models of reduce dimension are frequently used which take into account some physical considerations in order to study the transient stability of the synchronous machine and design a controller.

One of the most used model for designing a nonlinear controller is the so-called the one axes model. Assuming that the stator sub-transient dynamics and those of the transmission line are neglected, taking into account that T''_{qo}, T''_{do} and T'_{qo} are sufficiently small, and neglecting the dynamics driven the turbines assuming the mechanical torque T_M is constant, and taking into account the assumption that the impedance are constant and $X_q = X'_d$. Then, a 6th order model of the generator is represented by the following one axes model

$$\begin{cases} \dot{\delta} &= \omega - \omega_s \\ \dot{\omega} &= \frac{\omega_s}{2H}\left(P_m - D(\omega - \omega_s) - E'_{q_i} I_{q_i}\right) \\ \dot{E}'_q &= \frac{1}{T'_d}(E_f - E'_q - (X_d - X'_d)I_d) \end{cases} \tag{18.3}$$

with the linear algebraic relations:

$$0 = (R_s + R_e) Id - \left(X'_q + X_{ep}\right) I_q + V_s sin\left(\delta - \theta_{vs}\right) \tag{18.4}$$

$$0 = (R_s + R_e) Iq - \left(X'_d + X_{ep}\right) I_d - E'_q + V_s cos\left(\delta - \theta_{vs}\right) \tag{18.5}$$

where $T_e = E'_q I_q$, and $E_f(t)$ is the input of the system. Taking the system described by (18.1), the control problem can be formulated as follows:

Control objective: Considering the dynamical system (18.1) and using the only available information, design a control law $u(t)$ such that the rotor angle achieves the prescribed behavior with all the internal variables of the system being bounded. Then, in order to design a controller some assumptions are introduced.

Assumptions
A1. δ is available by measurement and the operating point (δ^*, 0, E'^*_q) is known.
A2. The mechanical power P_m is constant and known and all system parameters are known.
A3. No saturation in the model is considered.

18.2.3 Sliding-Mode Controller Design

Now, we introduce the most important results related to high order sliding mode which will be considered in the sequel (see [3], [4], for more details).

Consider systems belonging to a class of single-input-single-output systems with a known relative degree r, which are represented by

$$\dot{x} = f(x) + g(x)u, \qquad \sigma = \sigma(t,x) \tag{18.6}$$

where $x(t_0) = x_0$, $t_0 \geq 0$, $x \in B_x \subset \mathbb{R}^3$ is the *state vector*, $u \in \mathbb{R}^n$ is the *control input vector*, the field vectors f and g are assumed to be bounded with their components being smooth function of x and $\sigma : \mathbb{R}^{n+1} \to \mathbb{R}$ are unknown smooth functions. B_x denotes a closed and bounded subset, centered at the origin. In order to design a finite-time convergent controller some conditions are required. Since the relative degree r of the system is assumed to be constant and known, the control explicitly appears first time in rth total time derivative of σ and

$$\sigma^{(r)} = h(t,x) + m(t,x)u \tag{18.7}$$

where $h(t,x) = \sigma^{(r)}|_{u=0}$, $m(t,x) = (\partial/\partial u)\sigma(r) \neq 0$. It is supposed that for some $K_m, K_M, C > 0$

$$0 < K_m \leq \frac{\partial}{\partial u}\sigma^{(r)} \leq K_M \qquad |\sigma^{(r)}|_{u=0} \leq C \tag{18.8}$$

which is always true at least locally. From (18.7) and (18.8),

$$\sigma^{(r)} \in [-C, C] + [K_m, K_M]u \tag{18.9}$$

The closed differential inclusion is understood here in the Filippov sense, which means that the right-hand vector set is enlarged in a special way, in order to satisfy certain and semi-continuity conditions. The inclusion only requires to know the constants r, C, K_m and K_M of the system (18.6). These conditions allow to give a solution to this control problem (see [4]).

To design a high order sliding mode control for the system, we consider the following n-dimensional nonlinear surface defined by

$$\sigma(x, x^*) = 0 \tag{18.10}$$

where x^* is equilibrium point of the system and each function $\sigma_i : \mathbb{R}^3 \to \mathbb{R}, i = 1, ..., n$, is a C^1 function such that $\sigma_i(0) = 0$. Then, provided that successive total time derivatives σ, $\dot{\sigma}$, ...,$\sigma^{(r-1)}$ are continuous functions of the closed-system state-space variables, and

$$\sigma = \dot{\sigma} = ... = \sigma^{(r-1)} = 0 \tag{18.11}$$

is a nonempty integral set, the motion of (18.11) is called r-sliding mode. Under the above considerations the controller which will be designed for finite-time stabilization of smooth systems at an equilibrium point, is a quasi-continuous high order sliding mode controller, which is discontinuous at least (18.11), and $r-$ sliding homogeneous (see [3] and [4] for more details). This controller can be determined as follows. Let us $i = 0, ..., r-1$. Denote $\varphi_{0,r} = \sigma \quad N_{0,r} = |\sigma|, \quad \Psi_{0,r} = \varphi_{0,r}/N_{0,r} = sign\sigma$,

$$\varphi_{i,r} = \sigma^{(i)} + \beta_i N_{i-1,r}^{(r-i+1)} \Psi_{i-1,r} \tag{18.12}$$

$$N_{i,r} = |\sigma^{(i)}| + \beta_i N_{i-1,r}^{(r-i)/(r-i+1)} \tag{18.13}$$

$$\Psi_{i,r} = \varphi_{i,r}/N_{i,r} \tag{18.14}$$

where $\beta_i, ..., \beta_{r-1}$, α are positive numbers, which are chosen sufficiently large in the list order, the controller

$$u = -\alpha \Psi_{r-1,r}(\sigma, \dot{\sigma}, ..., \sigma^{r-1}) \tag{18.15}$$

is r-sliding homogeneous and provided for the finite-time stability, $\sigma = 0$. Each choice of parameters $\beta_1, ..., \beta_{r-1}$ determines a controller family applicable to all systems (21.13) of relative degree r.

18.2.3.1 Differentiator Design

It is clear that in order to implement the control law (18.15), it is necessary to know the real time exact calculation or direct measurement of $\sigma, \dot{\sigma}, \ddot{\sigma}$ or all components of the state vector. However, in order to reduce the number of sensors, the only measurable signal in the system is the rotor angle δ. Combining the controller (18.15) and the homogeneous differentiator (see [3]) given by

$$\begin{aligned}
\dot{z}_0 &= v_0 \\
v_0 &= -\lambda_r L^{1/r}|z_0-\sigma|^{(r-1)/r} sign(z_0-\sigma)+z_1 \\
&\vdots \\
\dot{z}_k &= v_k \\
v_k &= -\lambda_{r-k} L^{1/(r-k)}|z_k-v_{k-1}|^{(r-k-1)/(r-k)} sign(z_k-v_{k-1})+z_{k+1} \\
\dot{z}_{r-1} &= -\lambda_1 L sign(z_{r-1}-v_{r-2})
\end{aligned} \tag{18.16}$$

for k = 1,..., r-2; where z_0, z_1,..., z_k are estimates of the k-th derivatives of σ.

18.2.3.2 Sliding-Mode Control for SMIB Power Systems

Now, the proposed methodology is applied to the SMIB system (18.1) as shown in Figure 18.1. Since system (21.13) has relative degree equal to 3 and $x^* = (x_1^*, x_2^*, x_3^*)$ is a stable equilibrium point of system (21.13). Consider the following nonlinear switching surface defined by $\sigma(x,x^*) = x_1 - x_1^*$, where

$$\begin{aligned}
\dot{\sigma}(x,x^*) &= x_2 \\
\ddot{\sigma}(x,x^*) &= a_1 - a_2 x_2 - \frac{a_3}{a_4 + a_5(x_3 - a_6)} sin(x_1)
\end{aligned}$$

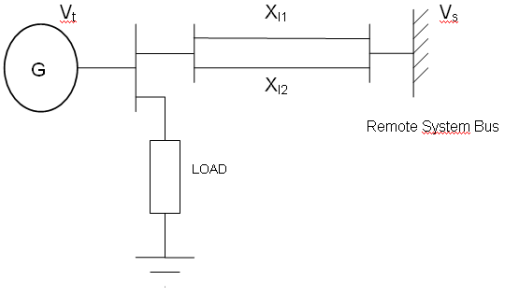

Fig. 18.1 Synchronous generator connected to a infinity bus.

Remark 18.1. It is clear that other switching surfaces can be defined.

Simulations results obtained using the following system parameters. Generator: $\omega_s = 377$ rad/s, $D = 0$, $H = 3.542$, $T_m = 0.6$ pu, $T'_{do} = 6.66$, $T'_{qo} = 0.44$, $T''_{do} = 0.03$, $T''_{qo} = 0.05$, $x_d = 1.7572$, $x_q = 1.5845$, $x'_d = 0.4245$, $x'_q = 1.04$, $x''_d = 0.25$, $x''_q = 0.25$, $Re = 0$. Infinite bus: $V_s = 1$. Transmission line: $R = 0$, $X_{l1} = 0.45$, $X_{l2} = 0.30$. For the differentiator: $\lambda_1 = 1.1$, $\lambda_2 = 1.5$, $\lambda_3 = 2$ and $L = 200$. Control input u_B: $\alpha_1 = 0.7$. Control input E_f : $\alpha_2 = -20$. The initial conditions were chosen as follows. $\delta_o = .744 rad$; $\omega_o = 377$ rad/s ; $E'_{qo} = 1.34$ p.u., $E'_{do} = 0.165$ p.u.; $\psi_{qo} = -0.48$ p.u.; $\psi_{do} = 1.109$ p.u. It is worth mentioning that the sliding-mode differentiator-controller is computed form the 3er model and it is implemented in the 6th order model.

The simulation results using the sliding mode control are shown in the Figure 18.2 and Figure 18.3, where we can appreciate the good performance of such controller under of the presence of a triphasic failure in the line. Notice that the controller stabilize all variables around the equilibrium point and damps out the angle oscillations. It is clear that the proposed scheme has a good performance inreducing overshoots and oscillations in few cycles.

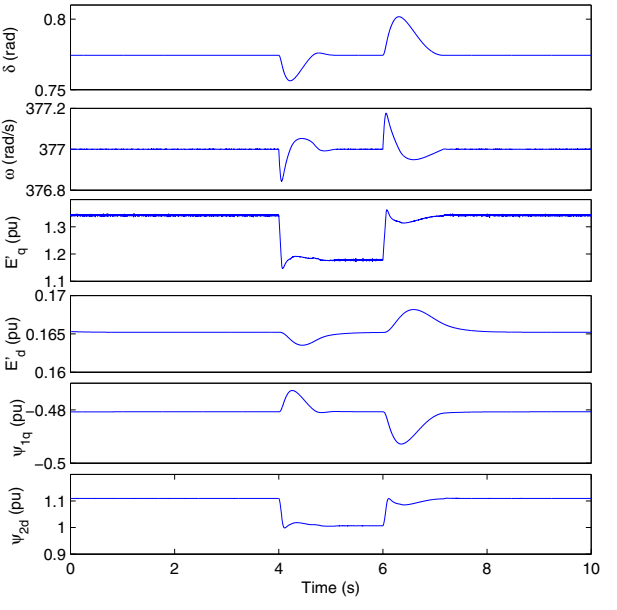

Fig. 18.2 Responses of the system in closed-loop.

18.2.4 Multi-machine Mathematical Model

Now, we study, under some standard assumptions, the dynamics of n interconnected generators through a transmission network can be described by the one axes model (21.13), (see [11]). The network has been reduced to internal bus representation assuming the loads to be constant impedances and taking into account the presence of transfer conductances. Then, the dynamical model of the i-th machine is represented by

$$\begin{cases} \dot{\delta}_i &= \omega_i - \omega_s \\ \dot{\omega}_i &= \frac{\omega_s}{2H_i}\left(P_{m_i} - D_i(\omega_i - \omega_s) - E'_{q_i} I_{q_i}\right) \\ \dot{E}'_{q_i} &= \frac{1}{T'_{d_i}}(E_{f_i} - E'_{q_i} - (X_{d_i} - X'_{d_i})I_{d_i}) \end{cases} \tag{18.17}$$

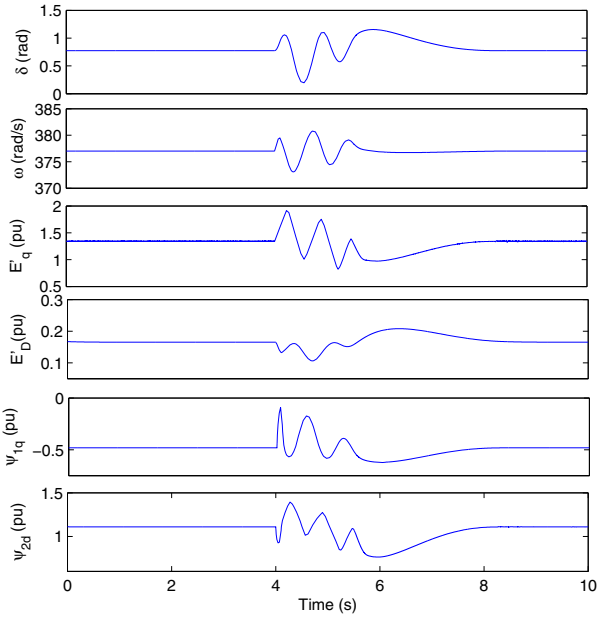

Fig. 18.3 Responses under triphasic failure.

where

$$I_{q_i} = G_{ii}E'_{q_i} + \sum_{j=1, j\neq i}^{n} E'_{q_j}\left\{G_{ij}cos(\delta_j - \delta_i) - B_{ij}sin(\delta_j - \delta_i)\right\}$$

$$I_{d_i} = -B_{ii}E'_{q_i} - \sum_{j=1, j\neq i}^{n} E'_{q_j}\left\{G_{ij}sin(\delta_j - \delta_i) + B_{ij}cos(\delta_j - \delta_i)\right\}$$

I_{q_i}, I_{d_i}	Currents in d-q reference frame of the i-th generator,
$E'_{q_i}(t)$	Transient EMF in the quadrature axis,
$E_{f_i}(t)$	The equivalent EMF in the excitation coil,
X_{d_i}, X'_{d_i}	Direct axis and direct axis transient reactance, respectively,
P_{m_i}	Mechanical input power,in p.u.
D_i	Damping factor; in p.u.
H_i	inertia constant, in seconds;
T'_{d_i}	Direct axis transient short circuit time constant, in seconds;
$\delta_i(t)$	Rotor angle, in radians;
$\omega_i(t)$	Relative speed,
$\omega_s = 2\pi f_s$	Synchronous machine speed, in rad/s;
G_{ij}, B_{ij}	$\{ij\}$ nodal conductance and susceptance matrices, respectively,

which are symmetric; at the internal nodes after eliminating all physical buses, in p.u.. Then, the state space representation of the multi-machine power system is given by

$$\begin{cases} \dot{x}_{i1} &= x_{i2} \\ \dot{x}_{i2} &= f_{i1}(X) \\ \dot{x}_{i3} &= f_{i2}(X) + u_i \end{cases}$$

where

$$f_{i1}(X) = a_i - b_i x_{i2} - c_i x_{i3}^2 - d_i x_{i3} \sum_{j=1, j\neq i}^{n} x_{j3} \left\{ G_{ij} cos(x_{j1} - x_{i1}) - B_{ij} sin(x_{j1} - x_{i1}) \right\}$$

$$f_{i2}(x) = -e_i x_{i3} + h_i \sum_{j=1, j\neq i}^{n} x_{j3} \left\{ G_{ij} sin(x_{j1} - x_{i1}) + B_{ij} cos(x_{j1} - x_{i1}) \right\}$$

$$\begin{array}{lll} a_i = (\omega_s/2H_i)P_{m_i}, & b_i = (\omega_s/2H_i)D_i, & c_i = (\omega_s/2H_i)G_{ii} \\ d_i = \omega_s/2H_i, & e_i = (1 + (X_{d_i} - X_{d_i}^{'})B_{ii})/T_{d_i}^{'}, & h_i = (X_{d_i} - X_{d_i}^{'})/T_{d_i}^{'} \end{array}$$

are the system parameters, $X_i = [x_{i1}, x_{i2}, x_{i3}]^T = [\delta_i(t), \omega_i(t), E_{q_i}^{'}(t)]^T$ for $i = 1, ..., n$, represents the state vector of i-th subsystem, thus $X = [X_1, X_2, ..., X_n]^T$ is the state vector of multi-machine system and the control inputs is given by $u_i = (1/T_{d_i}^{'})E_{fi}(t)$.

The control objective can be established as follows: Considering the model (18.17) and assuming that the currents $I_{q_i}(t)$ and $I_{d_i}(t)$ and the rotor angle $\delta_i(t)$ of each generator are available for measurement. Then, design a robust excitation control law for the system (18.17) in such a way the transient stability properties of system's operating point are guarantee improving its behavior under presence of noise in the measurable signals and faults in the network.

18.2.4.1 Sliding-Mode Control for Multi-machine Power Systems

Now, we design a control law for n interconnected machines based on sliding mode technique in such a way the stability properties of the system are improved. Since each subsystem (18.17) has relative degree equal to 3, then the resulting control law is given by

$$u = -\alpha \frac{\ddot{\sigma} + 2(|\dot{\sigma}| + |\sigma|^{2/3})^{-1/2}(\dot{\sigma} + |\sigma|^{2/3} sign\sigma)}{|\ddot{\sigma}| + 2(|\dot{\sigma}| + |\sigma|^2/3)1/2} \tag{18.18}$$

Now, considering the following nonlinear switching surface defined by $\sigma(X - X^*) = (\sigma_1(X - X^*), \sigma_2(X - X^*), \sigma_3(X - X^*))^T = 0$, where

$$\begin{aligned} \sigma_i(X) &= x_{i1} - x_{i1}^* \\ \dot{\sigma}_i(X) &= x_{i2} \\ \ddot{\sigma}_i(X) &= a_i - b_i x_{i2} - c_i x_{i3}^2 - d_i x_{i3} I_{qi} \end{aligned}$$

for $i = 1, 2, 3$, $X_i^* = (x_{i1}^*, x_{i2}^*, x_{i3}^*)$ is an equilibrium point.

Remark 18.2. It is worth noticing that the controller is expressed only in terms of local measurable variables (x_{i1}, x_{i2}, x_{i3}) and I_{qi} for $i = 1,2,3$. Consequently, the resulting controller is a decentralized output feedback (see [3], [14]).

Now, assuming that the only measurable signals in the system are the rotor angle δ_i, in order to reduce the number of sensors. Then, the control objective is to implement a finite-time convergent differentiator based on high order sliding mode, when the outputs $\sigma_i = \delta_i - \delta_i^*$ are available to estimate the values of $\dot{\sigma}_i$ and $\ddot{\sigma}_i$. The robust control law stabilizing the synchronous machine i, for $i = 1,2,3$; is given by

$$u_i = -\alpha_i \Psi_{r-1,r}(z_{i0}, z_{i1}, z_{i2}) \tag{18.19}$$

where z_{i0}, z_{i1}, and z_{i2} are given by the differentiator

$$\begin{aligned} \dot{z}_{i0} &= v_{i0} \\ v_{i0} &= -\lambda_{i3} L_i^{1/3} |z_{i0} - \sigma_i|^{2/3} sign(z_{i0} - \sigma_i) + z_{i1} \\ \dot{z}_{i1} &= v_{i1} \\ v_{i1} &= -\lambda_{i2} L_i^{1/2} |z_{i1} - v_{i0}|^{1/2} sign(z_{i1} - v_{i0}) + z_{i2} \\ \dot{z}_{i2} &= -\lambda_{i1} L_i sign(z_{i2} - v_{i1}) \end{aligned} \tag{18.20}$$

and the parameters of the differentiator (18.20) are chosen according to the condition $|\sigma_i^{(r)}| \leq L_i$, when L_i satisfies $L_i \geq C_i + \alpha_i K_M$. Finally, taken the following computer-tested values $\lambda_{i1} = 1.1$, $\lambda_{i2} = 1.5$ and $\lambda_{i3} = 2$ (see [3] for more details).

Notice that in the differentiator not appear the terms of interconnection, therefore the control scheme is completely decentralized. Furthermore, the order of the differentiator is not associated with number of machines interconnected in the network, it depends only on the relative degree of the model of the generator used for achieving the control objective. Furthermore, finite-time convergence of the observer allows to design the observer and the control law separately, i.e. the separation principle is satisfied.

18.2.4.2 Simulation Results

Now, we present some simulation results when the proposed scheme is implemented in a multi-machine system. In Figure 18.4 is shown the multi-machine system considered which represent a system of 3 generators interconnected. The numerical values of the generators parameters are presented in the Table 1.

Table 1 Generators parameters.

Parameter	Gen_1	Gen_2	Gen_3
$H(seg)$	23.64	6.4	3.01
$X_d(pu)$	0.146	0.8958	1.3125
$X'_d(pu)$	0.0608	0.1198	0.1813
$D(pu)$	0.3100	0.5350	0.6000
$P_m(pu)$	0.7157	1.6295	0.8502
$T'_{do}(seg)$	8.96	6.0	5.89

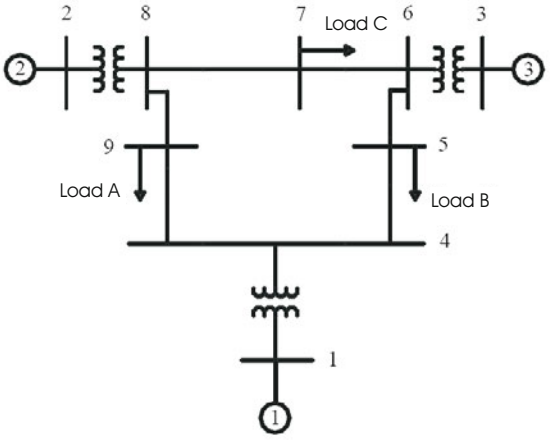

Fig. 18.4 Three-machine system.

Furthermore, the topology of the network has been represented by the conductance and susceptance nodal matrices

$$G = \begin{bmatrix} 0.8453 & 0.2870 & 0.2095 \\ 0.2870 & 0.4199 & 0.2132 \\ 0.2095 & 0.2132 & 0.2770 \end{bmatrix}, \qquad B = \begin{bmatrix} -2.9882 & 1.5130 & 1.2256 \\ 1.5130 & -2.7238 & 1.0879 \\ 1.2256 & 1.0879 & -2.3681 \end{bmatrix}$$

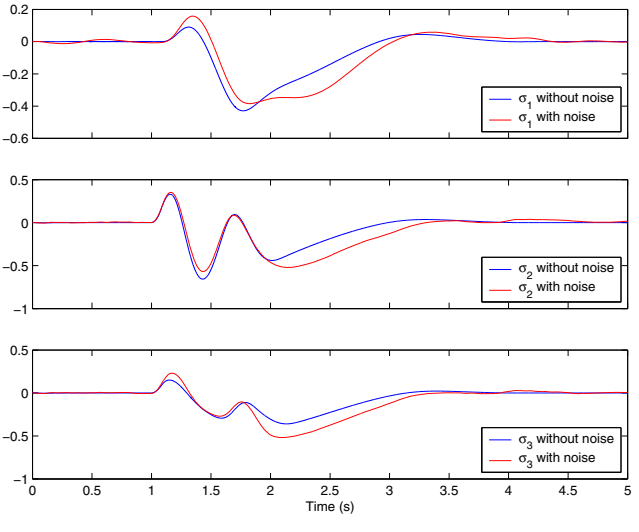

Fig. 18.5 Responses of the three-machine system.

In order to implement the controller, the following equilibrium point of the three-machine system is considered.

$$EP_1 : \begin{cases} x_{11}^* = 0.0396 \; x_{12}^* = 0 \; x_{13}^* = 1.0566 \\ x_{21}^* = 0.3444 \; x_{22}^* = 0 \; x_{23}^* = 1.0502 \\ x_{31}^* = 0.2300 \; x_{32}^* = 0 \; x_{33}^* = 1.017 \end{cases}$$

The parameters of the differentiators were selected as follows: $\lambda_{i1} = 1.1$, $\lambda_{i2} = 1.5$, $\lambda_{i3} = 2$, $L = 500$, for $i = 1, 2, 3$.

The performance of the proposed scheme is illustrated in Figure 18.5, where the responses of all state variables of the multi-machine system are shown. Notice that the good performance of the proposed controller has a better performance and stabilizes the machine variables and damps out the oscillations few cycles after.

18.3 Helicopter: Twin Rotor System

Helicopter is an aircraft that is lifted, propelled and maneuvered by vertical and horizontal rotors. All twin rotor aircrafts have high cross-coupling in all their degrees of motion. Especially the gyroscopic effect on azimuth dynamics prevents precise maneuvers by the operator emphasizing the need to compensate cross-coupling, a task that clearly adds to the workload for the pilot if done manually.

The twin rotor system recreates a simplified behavior of a real helicopter with fewer degrees of freedom. In real helicopters the control is generally achieved by tilting appropriately blades of the rotors with the collective and cyclic actuators, while keeping constant rotor speed. To simplify the mechanical design of the system, the twin rotor system setup considered in this presentation, is designed slightly differently. In this case, the blades of the rotors have a fixed angle of attack, and control is achieved by controlling the speeds of the rotors. As a consequence of this, the twin rotor system has highly nonlinear coupled dynamics. Additionally, it tends to be non-minimum phase system exhibiting unstable zero dynamics. This system poses very challenging problem of precise maneuvering in the presence of cross-coupling. It has been extensively investigated under the algorithms ranging from linear robust control to nonlinear control domains.

In this Section, the control objective is to design a robust controller for a twin rotor system taking into account the cross-couplings residing in the helicopter dynamics in such a way the improve its stability under external disturbances.

18.3.1 Dynamical Model of a Twin Rotor System

The dynamical model of the 2-DOF twin rotor system is described by the following equations

$$\begin{aligned}
\dot{x}_1 &= x_2 \\
\dot{x}_2 &= \frac{\left\{g\left[(A-B)\cos(x_1) - C\sin(x_1)\right] + l_m F_v - [A+B+C]\sin(x_1)\cos(x_1)x_4^2\right\}}{J_v} \\
&\quad - \frac{\{f_v x_2 - a_1|\omega_m|x_2 + k_{hv}u_h\}}{J_v} \\
\dot{x}_3 &= x_{i4} \\
\dot{x}_4 &= \frac{l_t F_h \cos(x_1) - f_h x_4 - a_2|\omega_t|x_4 + k_{vh}u_v}{D\sin(x_1)^2 + E\cos(x_1)^2 + F}
\end{aligned} \tag{18.22}$$

where $X = [x_1, ..., x_4]^T$ represents the state vector of the system such as $X = [\theta, \dot{\theta}, \psi, \dot{\psi}]$.
θ, ψ represent vertical and horizontal angles, respectively.
$\dot{\theta}, \dot{\psi}$ represent vertical and horizontal velocities.
A, B, C, D, E, F are inertial constants taken from experimental setup measures.
l_m, l_t are the lengths of the main and tail parts of the beam.
f_v, f_h are viscous friction terms relative to vertical and horizontal axes.
ω_m, ω_t are angular velocities from main and tail rotors. Relationship has been experimentally determined, depends on the input voltage.
J_v is the sum of moments of inertia relative to the horizontal axis.
F_v, F_h denote the dependence of the propulsive force on the angular velocity of the main and tail rotors (experimentally determined).
a_1, a_2 are model constants.
k_{hv} and k_{vh} represent cross-coupling constant terms.
u_v and u_h represent the voltage applied to motors.
The angles θ and ψ are the measurable outputs.
Velocities $\dot{\theta}$ and $\dot{\psi}$ are assumed to be non-measurable states.

In the control system and robotic communities have gained interest for the development of observers applied to UAVs due to the important developments of embedded electronics and micro-controllers. This technological improvement has motivated the testing of more sophisticated algorithms in real time.

Motivated by previous arguments, in what follows a differentiator will be designed in order to solve the problem of speed estimation of a twin rotor system, when the vertical and horizontal angles are available from measurements.

18.3.1.1 Observer Design

Form the model (18.22), and knowing that the outputs of the system $y_1 = x_1$ and $y_2 = x_3$ are measurable, we use a differentiator in order to estimate the non measurable state components. For that

$$\begin{aligned}
\dot{z}_{i,0} &= \nu_{i,0} \\
\nu_{i,0} &= -\lambda_{i,2} L_i^{1/2} |z_{i,0} - \sigma_i|^{1/2} sign\left(z_{i,0} - \sigma_i\right) + z_{i,1} \\
\dot{z}_{i,1} &= -\lambda_{i,1} L_i sign\left(z_{i,1} - \nu_{i,0}\right)
\end{aligned} \tag{18.23}$$

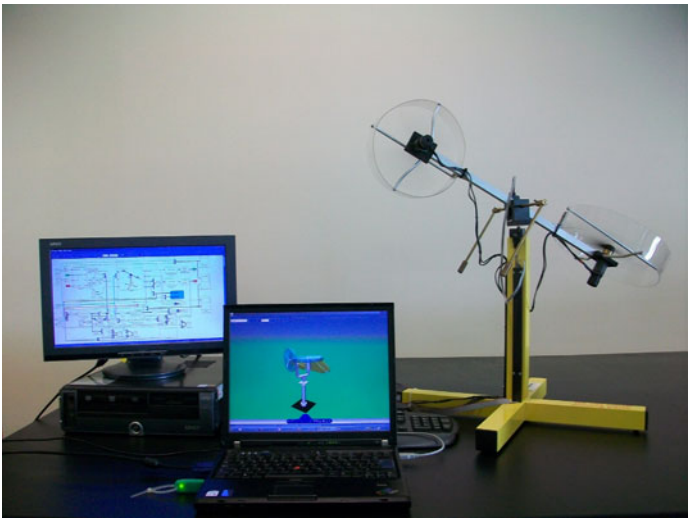

Fig. 18.6 Helicopter: twin rotor system setup.

for $i = 1, 2$. Then, the controller is of the form.

$$u_i = -\alpha_i sign(z_{i,1}) + |z_{i,0}|^{1/2} sign(z_{i,0})) \tag{18.24}$$

where $u_1 = u_h$ and $u_2 = u_v$.

18.3.1.2 Simulation Results

In this Section, we provide simulation results to illustrate the effectiveness of the proposed methodology when applied to the twin rotor systems.

The case of study concerns the design of a robust control for twin rotor system of a 2-DOF helicopter setup (see Figure 18.6).

Platform consists of a beam pivoted on its base in such a way that it can rotate freely both in the horizontal and vertical planes. At both ends of the beam there are rotors (main and tail rotors) driven by DC motors. A counterbalance arm with a weight at its end is fixed to the beam at the pivot. The state of the beam is described by four process variables: horizontal and vertical angles measured by position sensors fitted at the pivot, and two corresponding angular velocities. Two additional state variables are the angular velocities of the rotors, measured by tacho-generators coupled with the driving DC motors.

The numerical values from the system parameters were $J_v = 0.02421, m = 0.5920, l_m = 0.202, l_t = 0.216, g = 9.8, A = 1.0671, B = 1.4678, C = 0.0044, D = 0.0006225, E = 0.0224, F = 0.0021, f_v = 45, f_h = 90, a_1 = 0.1, a_2 = 0.1, k_{vh} = 20, k_{hv} = 18$.

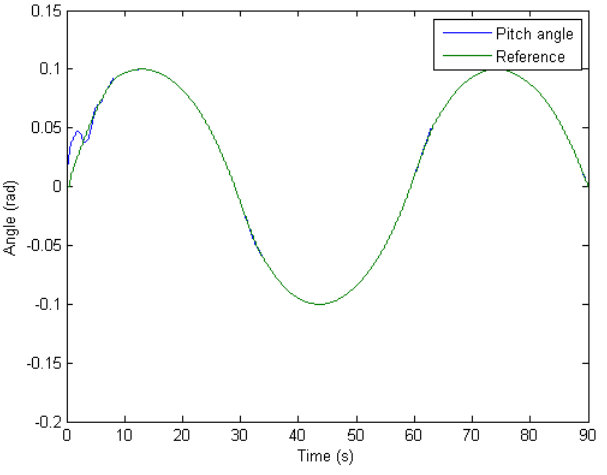

Fig. 18.7 Reference and horizontal response of helicopter system with 2-DOF.

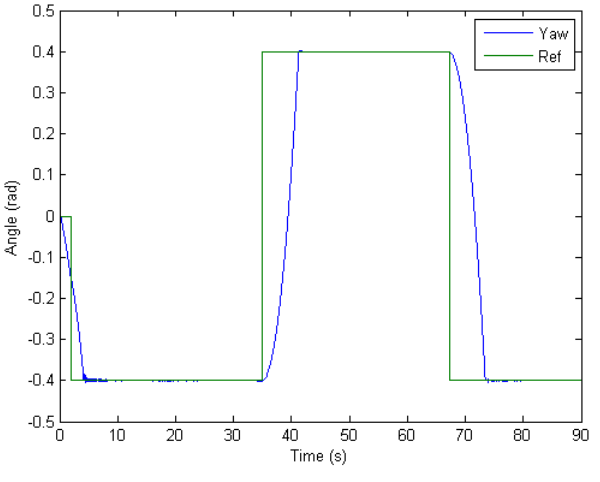

Fig. 18.8 Reference and vertical response of helicopter system with 2-DOF.

Defining $\sigma_1 = y1 - y_{ref,1}$ and $\sigma_1 = y3 - y_{ref,2}$, where $y_{ref,1} = 0.1sin(wt)$ of 1/60 Hz frequency and $y_{ref,2} = 0.4Square(t)$ of 1/0.015 Hz frequency. Assuming the helicopter starts moving from a rest point, initial value of the states variables were $x_1(0) = 0.01$, $x_3(0) = 0.01$, $x_2(0) = 0.01$, $x_4(0) = 0.01$. Furthermore, the differentiator parameters were chosen as follows: $\lambda_{1,1} = 1.5$, $\lambda_{1,2} = 1.1$, $\lambda_{2,1} = 1.85$, $\lambda_{2,2} = 1.81$, $L_1 = 20$, $L_2 = 20$. Finally, the control parameters were chosen as follows: $\alpha_1 = 18.02$, $\alpha_2 = 450.02$.

In Figure 18.7 and Figure 18.8 are plotted the responses of vertical and horizontal angles, respectively; tracking the desired reference and which are obtained from the twin rotor system setup. In all simulations, we can see that the output controller tracks the desired time varying references of the horizontal and vertical angles. Furthermore, we can see that the position and speed converges to the desired references in finite-time. It is clear that the proposed controller has a good performance in terms of rate of convergence.

18.4 Teleoperation Bilateral: Master-Slave Systems

18.4.1 Introduction

Recently, the application of nonlinear control theory has attracted the attention of the research community to understand and overcome problems in bilateral teleoperation. Furthermore, teleoperation over the internet has introduced new problems due to the effects of delays in communications, which may cause instability in the system.

In a system which is teleoperated basically, a human operator interacts with an interface, called master teleoperator, and drives it in order to govern the remote counterpart, on the opposite side, while another interface (slave operator) is in charge of directly implementing commands received from the operator on the remote environment (see [8], [9]).

Several teleoperation schemes considering time-delays have been proposed in the last decades. However, stability problems have found in these schemes, so that important improvements have been suggested. Recently, an increased interest on sliding-mode control has been developed to address the problem of delays in teleoperation, which has generated and inspired a line of research in designing controllers to compensate the effects of these delays in real time (see [26] [27], [25]).

The control objective is to design a robust control for a teleoperator system taking into account a fixe delay time in the communication system. The scheme applied contains an impedance control for the master system combined with a second order sliding mode control and differentiator for the slave system. Thus, this scheme provides a better performance over a wide range of constant time-delays.

18.4.2 Teleoperation System

In a teleoperation general setting, the human imposes a force on the master manipulator which in turn results in a displacement that is transmitted to the slave that mimics that movement. If the slave possess force sensors, then it can reflect or transmit back to the master reaction forces from the task being performed, which enters into the input torque of the master, and the teleoperator is said to be controlled bilaterally.

For sake of simplicity, we consider the dynamics of the 1-DOF master/slave systems are represented as a mass-damper system

$$M_m\ddot{x}_m(t) + C_m\dot{x}_m(t) = u_m(t) + f_h(t) \tag{18.25}$$

$$M_s\ddot{x}_s(t) + C_s\dot{x}_s(t) = u_s(t) - f_e(t) \tag{18.26}$$

where x and u denote the position and the input torque, respectively; subscript m and s denote the master and the slave; f_h and f_e are the force applied at the master by the human operator, and the force exerted on the slave by the environment, respectively. Also M_i and C_i represent mass and viscous friction coefficient, respectively, with $i = m,s$ denoting master and slave. Furthermore, a time delay imposed on the communication channels is assumed to be constant and unknown.

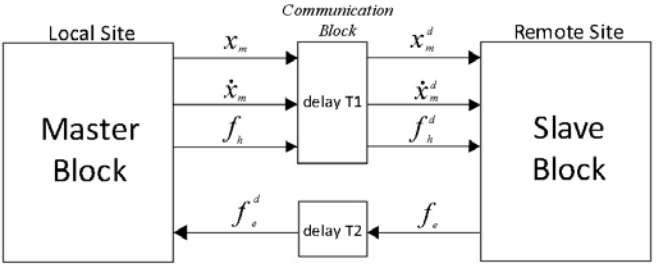

Fig. 18.9 A block diagram of bilateral teleoperation

This bilateral teleoperation system scheme can be represented by the block diagram shown in Figure 18.9. Furthermore, the position and force of the master are transmitted to the slave and the contact force of the slave is sent to the master through the communication channel, where there is a time delay in the communication channel. The signals from and to the channel are related as

$$\begin{aligned} x_m^d(t) &= x_m(t - T_1) & f_h^d(t) &= f_h(t - T_1) \\ \dot{x}_m^d(t) &:= \dot{x}_m(t - T_1) & f_e^d(t) &:= f_e(t - T_2) \end{aligned} \tag{18.27}$$

where x_m^d, $\dot{x}_m^d$, and f_h^d are the position and velocity of the master, and the force exerted by a human operator, respectively, which are transmitted to the slave through the communication channel; f_e^d is the external force at the slave transmitted to the slave through the master; T_1 is a time delay of the signal flowing from master to the slave, and T_2 is in the opposite direction.

This delayed signals out of the communication block are then scaled up or down by some factors, then the position/velocity command to the slave and the force signal to the master are modified such that $x_s = K_p x_m^d$ and $f_h = K_f f_e^d$, where K_p and K_f are position and force scale factors, respectively. Then, the state space representation of (18.25) and (18.26) are given as follows.

$$\begin{cases} \dot{x}_{m1} = x_{m2} \\ \dot{x}_{m2} = -\frac{C_m}{M_m} x_{m2} + \frac{1}{M_m} u_m + \frac{1}{M_m} f_h \end{cases} \tag{18.28}$$

$$\begin{cases} \dot{x}_{s1} = x_{s2} \\ \dot{x}_{s2} = -\frac{C_s}{M_s} x_{s2} + \frac{1}{M_s} u_s - \frac{1}{M_s} f_e \end{cases} \tag{18.29}$$

In what follows, a robust impedance controller as well as a differentiator in order to estimate the speed and acceleration are designed. It is clear that an extension of theses results for the multi-variable case can be obtained.

18.4.3 Controller Design

Now, an impedance controller and a sliding-mode based impedance controller are designed for the master and the slave, respectively.

Consider the following master control structure

$$u_m = -f_h + C_m \dot{x}_m + \frac{M_m}{\bar{M}_m}(f_h - K_f f_e^d - \bar{C}_m \dot{x}_m - \bar{K}_m x_m) \tag{18.30}$$

where $\bar{M}_m$, $\bar{C}_m$, $\bar{K}_m > 0$ are desired inertia, damping coefficient, and stiffness, respectively; of a desired impedance. Substituting (18.30) into (18.25), the closed-loop impedance error is given by

$$\bar{M}_m \ddot{x}_m + \bar{C}_m \dot{x}_m + \bar{K}_m x_m = f_h - K_f f_e^d \tag{18.31}$$

Consider the slave control design based on second order sliding mode approach to produce a desired impedance behavior modulated by the environmental contact force and robust to unknown time-delay. To this end, consider the desired slave impedance

$$\bar{M}_s \ddot{\tilde{x}}_s + \bar{C}_s \dot{\tilde{x}}_s + \bar{K}_s \tilde{x}_s = -f_e \tag{18.32}$$

where $\bar{M}_s$, $\bar{C}_s$, $\bar{K}_s > 0$ are the desired inertia, damping, and stiffness, respectively, and $\ddot{\tilde{x}}_s := \ddot{x}_s - K_p \ddot{x}_m^d$, $\dot{\tilde{x}}_s := \dot{x}_s - K_p \dot{x}_m^d$, $\tilde{x}_s := x_s - K_p x_m^d$ are the slave tracking errors for acceleration, velocity and position, respectively.

Since we want to obtain (18.32) in closed-loop, then defining the following sliding surface

$$I_e = \bar{M}_s \ddot{\tilde{x}}_s + \bar{C}_s \dot{\tilde{x}}_s + \bar{K}_s \tilde{x}_s + f_e = 0 \tag{18.33}$$

Now, let us define the extended error variable as follows

$$\Omega = \frac{1}{\bar{m}_s} \left[\int_0^t I_e(\tau) d\tau + K_i \int_0^t \int_0^\sigma sign(I_e(\tau)) d\tau d\sigma \right] \tag{18.34}$$

where $K_i > 0$ is the sliding mode gain. Substituting (18.33) into (18.34) and integrating, we finally obtain

$$\Omega = \dot{\tilde{x}}_s + \frac{\bar{C}_s}{\bar{M}_s}\tilde{x}_s + \frac{1}{\bar{M}_s}\int_0^t [\bar{K}_s\tilde{x}_s + f_e]d\tau + \frac{K_i}{\bar{M}_s}\int_0^t\int_0^\sigma sign(I_e(\tau))d\tau d\sigma \tag{18.35}$$

The slave controller u_s has the following form

$$\begin{array}{l} u_s = -\frac{M_s}{\bar{M}_s}\left(\bar{C}_s\dot{\tilde{x}}_s + \bar{K}_s\tilde{x}_s + f_e + K_i\int_0^t sign(I_e(\tau))d\tau\right) \\ \quad + \frac{M_s}{\bar{M}_m}kK_p\left(f_h^d - K_f f_e^{dd} - \bar{C}_m\dot{x}_m^d - \bar{K}_m x_m^d\right) + f_e + C_s\dot{x}_s - K_g\Omega \end{array} \tag{18.36}$$

where $f_e^{dd} = f_e(t-2T)$, the superscript dd stands for the round trip delay: $2T$, $K_g > 0$, and $sign(\cdot)$ is the discontinuous signum function. The term $K_g\Omega$ has been added to achieve stability as it will be seen afterwards. Also, notice that (18.35) requires acceleration measurement because I_e depends on acceleration. To deal with this inconvenience, acceleration and velocity are estimated, at master and slave sides, by means of super twisting observers.

18.4.4 Super Twisting Observer Design

The elimination of sensors to measure velocity and acceleration is an advantage in robotics because expensive and bulky tachometers are avoided. Then, to reduce the number of sensors we add to the control scheme a nonlinear super twisting sliding mode observer (see [6]). This sliding mode observer is based on structural conditions and the iterative use of the super twisting algorithm. The importance of such observer is that it can be used as a tool to solve several difficult problems of observation.

Now, a finite time observer for slave system (18.29) is designed. Consider the following canonical form.

$$\begin{cases} \dot{x}_1 = x_2 \\ \dot{x}_2 = F(x_1, x_2, u, y) \end{cases} \tag{18.37}$$

with $F(x_1,x_2,u,y) = -\frac{C_s}{M_s}x_2 + \frac{1}{M_s}u_s - \frac{1}{M_s}f_h$.

Notice that the term F can be seen as unknown input, which must be estimate in such a way to estimate the acceleration of the slave system.

The super twisting observer for system (18.37) has the following form

$$\begin{array}{l} \dot{\hat{x}}_1 = \tilde{x}_2 + \lambda_1\sqrt{|\tilde{x}_1 - \hat{x}_1|}sign(\tilde{x}_1 - \hat{x}_1) \\ \dot{\tilde{x}}_2 = \alpha_1 sing(\tilde{x}_1 - \hat{x}_1) \\ \dot{\hat{x}}_2 = E_1[\tilde{\Theta} + \lambda_2(\sqrt{|\tilde{x}_2 - \hat{x}_2|})sign(\tilde{x}_2 - \hat{x}_2)] \\ \dot{\tilde{\Theta}} = E_2\alpha_2 sign(\tilde{x}_2 - \hat{x}_2) \end{array} \tag{18.38}$$

where α_1 and α_2 are the observer gains, λ_1 and λ_2 are the corrections factors designed for convergence of the estimation error, which are defined as $e_i = \tilde{x}_i - \hat{x}_i$, for $i = 1,2$. Also the scalar functions E_i for $i = 1,2$ are defined as: $E_i = 1$ if $e_i \leq \varepsilon_i$, else $E_i = 0$, where ε_i are small positive constants.

18.4.5 Simulation Results

Simulation results are obtained using the following parameter values. The parameter values of the each system are the following. Master System: $C_m = 0.9$, $M_m = 1.9$, $\bar{M}_m = 1.8641$, $\bar{C}_m = 1.5$, $K_f = .9$, $\bar{K}_m = 0.01$. Slave system: $C_s = 0.9$, $M_s = 7$, $\bar{C}_s = 0.5$, $\bar{M}_s = 0.3$, $\bar{K}_s = 15$. The parameters of the controller: $K_p = 1$, $K_g = 500$, $K_i = 0.1$, and the observer: $\alpha_1 = 100$, $\alpha_2 = 200$, $\lambda_1 = 10$, $\lambda_2 = 750$, $E_1 = 1$, $E_2 = 0$.

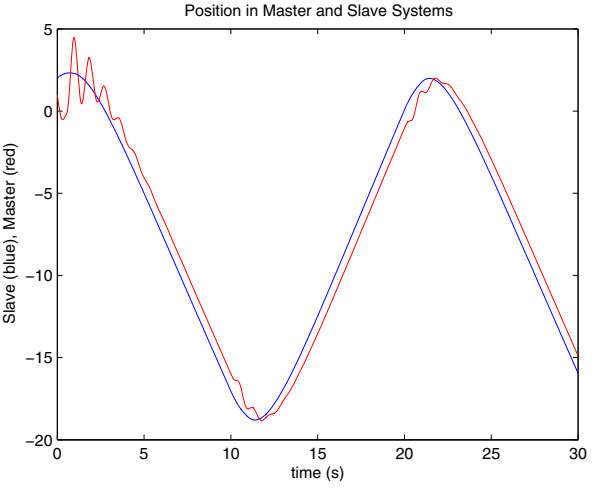

Fig. 18.10 Position responses of Master-Slave system.

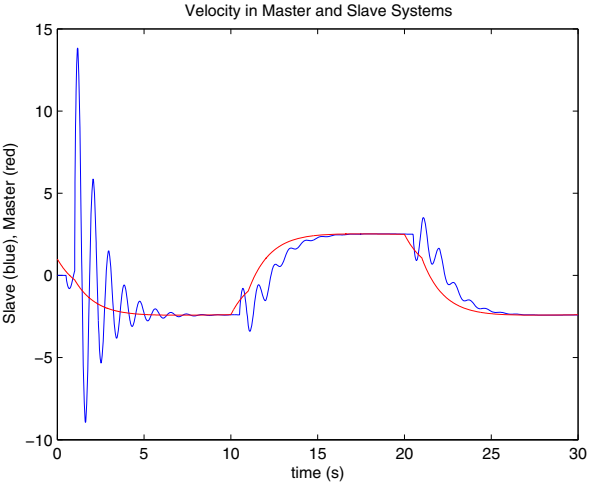

Fig. 18.11 Velocity responses of Master-Slave system.

In Figure 18.10 and Figure 18.11, the position and velocity responses are plotted. We can see the performance of the control when the master system tracks a desired trajectory and the slave system tracks the master system signal sent by the communication system with a time delay T, which was chosen of $T = 0.5$sec..

18.5 Conclusions

In this paper, an overview about the strategies of control and observation based on sliding modes techniques has been presented and implemented in electrical power systems (synchronous machine and multi-machines systems), in a twin rotor system (Helicopter of 2-DOF), and in a master-slave teleoperated bilaterally system, which are the research fields of the Mechatronics laboratory of the Universidad Autónoma de Nuevo León, in the CIIDIT-UANL Research Institute.

Furthermore, in all applications presented in this paper, the tested control-observer strategies based on sliding mode have been demonstrated the good performance as well as the finite-time convergence and robustness under external disturbances.

Acknowledgements. The author gratefully acknowledges the financial support by the Mexican CONACyT (Consejo Nacional de Ciencia y Tecnología) grant number 105799, by the FONCyT (Fondo Nacional para la Ciencia y la Tecnología) project number 93302.

References

1. Cho, H.C., Park, J.H.: Stable bilateral teleoperator under a time delay using a robust impedance control. Mechatronics 15, 611–625 (2005)
2. Young, K.D., Utkin, V., Özgüner, Ü.: A control engineer's guide to sliding mode control. IEEE Transactions on Control Systems Technology 7(3) (May 1999)
3. Levant, A.: High-order sliding modes, differentiation and output feedback control. Int. J. Control 76(9/10), 924–941 (2003)
4. Levant, A.: Quasi-continuous high order sliding-mode controllers. IEEE Transactions on Automatic Control 50(11), 1812–1816 (2005)
5. Davila, J., Fridman, L., Poznyak, A.: Observation and identification of mechanical systems via second order sliding modes. In: International workshop on variable structure systems, Aleghero, Italy, June 5 -7, pp. 232–237 (2006)
6. Floquet, T., Barbot, J.P.: Super twisting algorithm based step-by-step sliding mode observers nonlinear systems with unknown inputs. International Journal of Systems Science 38(10), 803–815 (2007)
7. Walcott, B.L., Żak, S.H.: State observation of nonlinear uncertain dynamical systems. IEEE Transactions on Automatic Control 32, 88–104 (1987)
8. Slotine, J.J., Hedrick, J.K., Misawa, E.A.: On sliding observers for nonlinear systems. ASME Journal Dynamical Systems Measurement Control 109, 245–252 (1987)
9. Hoyakem, P.F., Spong, M.W.: Bilateral Teleoperation: An historical survey. Automatica 42, 2035–2057 (2006)
10. Li, C., Elbuluk, M.: A sliding mode observer for sensorless control of permanent magnet synchronous motors. In: Industry Applications Conference (2001)

11. Bergen, A.: Power System Analysis. Prentice-Hall, Englewood Cliffs (1986)
12. Utkin, V.I., Guldner, J., Shi, J.: Sliding mode control in electromechanical systems. Taylor & Francis, Abington (1999)
13. Utkin, V.I.: Sliding modes in control and optimization. Comunications and Control Engineering Series. Springer, Heidelberg (1992)
14. Chapman, J.W., Ilic, M.D., King, C.A., Eng, L., Kaufman, H.: Stabilizing a multimachine power system via decentralized feedback linearizing excitation control. IEEE Trans. on Power Systems 8(1), 830–839 (1993)
15. Ortega, R., Galaz, M., Astolfi, A., Sun, Y., Shen, T.: Transient stabilization of multimachine power systems with nontrivial transfer conductances. IEEE Trans. on Automatic Control 50(1), 60–75 (2005)
16. Taore, D., Plestan, F., Glumineau, A., de Leon, J.: Sensroless induction motor: Hihg sliding mode controller and adaptive interconnected observer. IEEE Trans. Ind. Electron 55(1), 3818–3827 (2008)
17. Colbia-Vega, A., de Leon-Morales, J., Fridman, L., Salas-Pena, O., Mata-Jimenez, M.T.: Robust excitation control design using sliding-mode technique for multimachine power systems. Electric Power Systems Research 78(1), 1627–1634 (2008)
18. Loukianov, A.G., Caedo, J.M., Utkin, V.I., Cabrera-Vazquez, J.: Discontinuous Controller for Power System: Sliding-Mode Block Control Approach. IEEE Trans. On Industrial Electronics 51(2), 340–353 (2004)
19. Valavanis, K.P.: Advances in Unmanned Aerial Vehicle, University of south Florida Tampa, Florida. Springer, Heidelberg (2007)
20. Stengel, R.: Flight Dynamics, November 2004. Princeton University Press, Princeton (2004)
21. Zyskowky, M.K.: Aircraft Simulation Techniques Used in Low-Cost, Commercial Software. In: AIAA 2003, vol. 5818 (August 2003)
22. Melin, T.: A Vortex Lattice Matlab Implementation for linear Aerodynamic Wing Applications. Masters Thesis, Royal Institute of Technology, KTH (2000)
23. Etkin, B.: Dynamics of Flight Stability and Control, 3rd edn. John Wiley and Sons, Inc., Chichester (1996)
24. Naveed, U., Whidborne, J.F.: A lateral Directional Flight Control System for the MOB Blended Wing Body. Departament of Aerospace Sciences. Cranfield University, Bedfordshire MK45 OAL, UK
25. Guerra-Torres, C., de Leon-Morales, J., Glumineau, A., Traore, D., Boisliveau, R.: Teleoperation of an Experimental Platform of Electrical Machines through the Internet. International Journal of Online Engineering (iJOE) 42(1) (2121) ISSN 1861-2121
26. Garcia-Valdovinos, L.G., Parra-Vega, V., Arteaga, M.: Higher-order sliding mode impedance bilateral teleoperation with robust state estimation under constant unknown time delay. In: Proceedings IEEE/ASME Int. Conf. on Advanced Intelligent Mechatronics, pp. 1293–1298 (2005)
27. Cho, H.C., Park, J.H.: Stable bilateral teleoperatin under a time delay using a robuste impedance control. Mechatronics 15, 611–625 (2005)
28. Rodriguez, A., De Leon, J., Fridman, L.: Quasi-continuous high-order sliding-mode controllers for reduced-order chaos synchronization. International Journal of Non-Linear Mechanics 43, 948–961 (2008)
29. Rodriguez, A., De Leon, J., Fridman, L.: Synchronization in reduced-order of chaotic systems via control approaches based on high-order sliding-mode observer. Chaos, Solitons and Fractals 42, 3219–3233 (2009)